Bulletin of the Seismological Society of America, Vol. 100, No. 5A, pp. 2287–2292, October 2010, doi: 10.1785/0120090370

Short Note

Possibility of Biases in the Estimation of Earthquake Recurrence and Seismic Hazard from Geologic Data

by Steven G. Wesnousky

Abstract Aseismic deformation is an integral part of the earthquake process and may lead to systematic biases in the estimation of earthquake size, recurrence, and attendant strong ground motions in seismic hazard analyses founded on the geologic description of the locations, lengths, and slip rates of active faults. Observations are reviewed and presented to suggest that large earthquakes systematically rupture to increasingly greater depths below the seismogenic layer and that the portion of slip on faults accommodated by aseismic processes may be inversely related to the length of rupture expected to occur on them. If so, the expected seismic moment per unit area of earthquakes on mapped faults may be systematically overestimated as a function of rupture length when derived from regressions of seismic moment and aftershock area, and estimates of seismic moment rate derived from geologic measures of fault offset might be systematically overestimated as an inverse function of the length of rupture expected to recur on a fault.

Introduction

Regional seismic hazard analyses are now to varying degrees constructed on fault models that describe the slip rate, length, and width of earthquake producing faults across a region. The premise for the approach has developed over the last ~25 years (Wesnousky *et al.*, 1984; Wesnousky, 1986; Frankel *et al.*, 2002; Petersen *et al.*, 2007; Field *et al.*, 2009). When not derived directly from stratigraphic and structural relationships exposed in trenches excavated across mapped faults, the return times, T, of earthquakes on faults are estimated by dividing either the expected coseismic slip (U^{exp}) on a fault by the geologists' or geodecists' estimate of fault slip rate $\dot{U}^{\mathrm{geo}}$ or, equivalently, the expected seismic moment M_0^{exp} by the seismic moment rate $\dot{M}_0$. The coseismic slip U^{exp} and seismic moment M_0^{exp} of the expected earthquake are generally estimated from empirical regressions relating fault rupture length or area to the respective parameters from historical observations (e.g., Fig. 1; Wells and Coppersmith, 1994). The seismic moment rate $\dot{M}_0$ is equal to $\mu L W \dot{U}^{\mathrm{geo}}$, where L and W are the dimensions of the fault, and μ is crustal rigidity (Aki and Richards, 1980). Whereas aseismic deformation is recognized to be a fundamental part of the earthquake process, the possibility of systematics to the process has generally not been considered in seismic hazard analyses. In this note, I put forth some observations to suggest that aseismic deformation may be leading to systematic biases in current estimates of seismic hazard and may go toward resolving some issues that currently exist in seismic hazard analysis.

The Issues

The prediction of the size and frequency of earthquakes from geology is generally calibrated or checked by comparing the rate of seismicity predicted from a regional fault model to what has been observed historically (Fig. 2; Wesnousky *et al.*, 1983; Field *et al.*, 2008). While the approach has served well, there are two problems that arise in its application to the development of seismic hazard maps considered here. The first of these is that predictions of seismicity from geologic data tend to overestimate the number of moderate-sized events in a region as compared to what is observed. This has been true for more than 20 yr and apparently remains a problem today (Wesnousky *et al.*, 1984; Wesnousky, 1986; Field *et al.*, 2008, 2009). The mismatch has been referred to as the bulge (Field *et al.*, 2008; Fig. 2). The second problem is that existing fault models require that the amount of average slip per unit area on a fault plane systematically increases with rupture length, a prediction unsupported by instrumental seismological analyses. To avoid that increase in the amount of average slip per unit area and a concomitant increase in predicted long-period strong

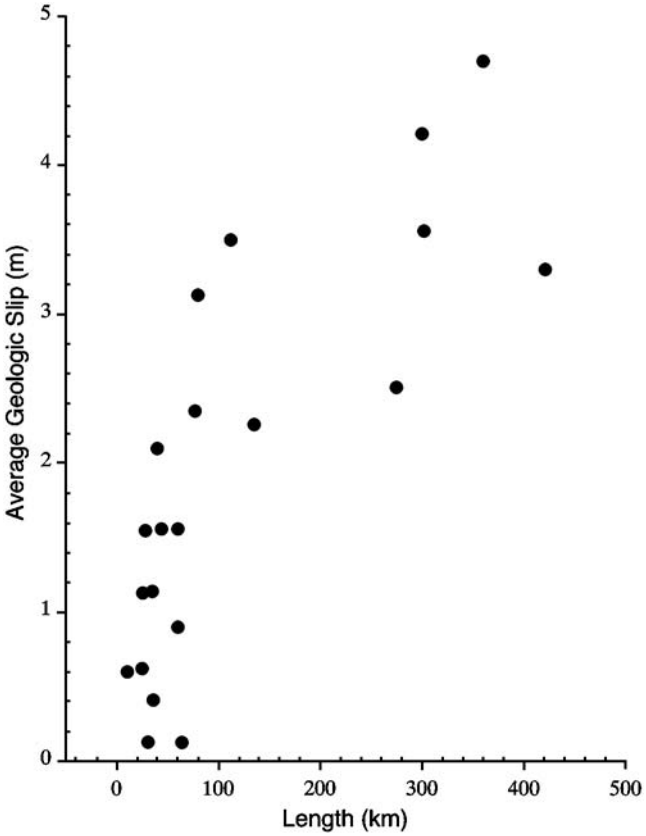

Figure 1. Example of empirical correlation of earthquake size to fault dimension. In this case, average surface displacement is plotted as a function of surface rupture length for continental strike-slip earthquakes (adapted from Wesnousky, 2008).

ground motions, physics-based numerical models of earthquake rupture are generally required to allow a relatively greater down-dip extent of rupture than used for the respective modeled faults (Somerville, 2006; Graves*et al.*, 2010; Graves, personal communication, 2009). So there is an internal inconsistency between the depth dimensions used in fault models to predict earthquake recurrence and those required for prediction of strong ground motions from physics-based numerical models.

The Base of the Seismogenic Layer and the Estimation of Earthquake Size and Strong Ground Motions from Fault Data

The observation that coseismic slip in large strike-slip earthquakes increases with rupture length (Fig. 1) was recently revisited by King and Wesnousky (2007). The particular observation results in a conundrum whereby calculations of static stress drop of large earthquakes increase with rupture length, a prediction that has not been borne out by seismological observation. The conundrum arises because elasticity models show stress drop is proportional to the average displacement on a fault divided by the shortest dimension of the fault, and, as generally assumed, that the shortest dimension of a fault is equal to the depth to which seismicity

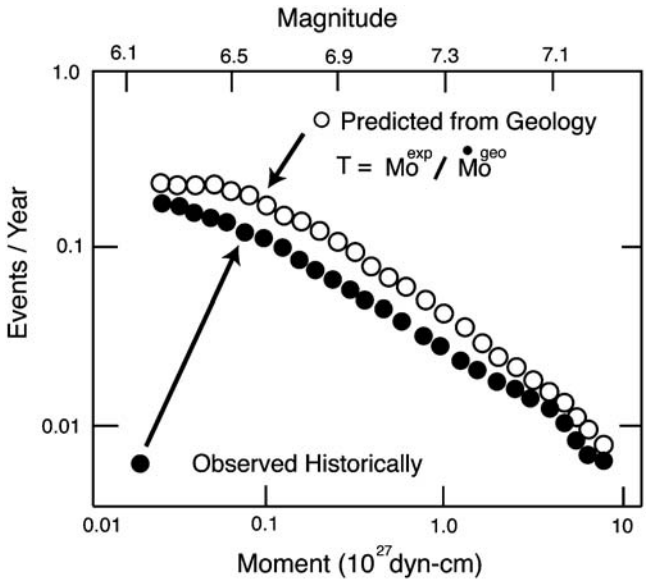

Figure 2. Schematic illustration of the manner in which predictions of seismicity from geologic fault models are calibrated to historical observations in magnitude-frequency plots. The seismicity emanating from a regional set of faults is typically estimated from each mapped fault with the assumption that the return time T of earthquakes on each mapped fault is equal to the seismic moment of the earthquake expected $M_0^{\exp}$ on the fault divided by the estimated seismic moment rate $\dot{M}_0$ for each fault. The size of the expected earthquake $M_0^{\exp}$ is taken from modern empirical regressions relating fault dimension to seismic moment, and the seismic moment rate $\dot{M}_0$ is proportional to the geologically determined fault slip rate $\dot{U}^{\text{geo}}$. It is common that more moderate-sized events are predicted from geologic fault models than observed (exaggerated here for clarity of illustration). The mismatch of the observed to the predicted number of earthquakes per year at moderate magnitudes has been referred to as the bulge.

is observed (the seismogenic layer), about 15 km in continental environments. It was shown that the conundrum can be resolved by assuming (1) a simple displacement-depth function of tapered and self-similar form that better reflects observation and is consistent with frictional models of fault behavior, and (2) it is allowed that larger earthquakes progressively rupture a greater amount below the seismogenic layer into a region of stable sliding, where rupture may propagate but not initiate. The static model then leads to prediction of constant stress drop and self-similarity for earthquakes across the entire spectrum of earthquake sizes. Since that time, physics-based models have yielded the same result (Hillers and Wesnousky, 2008; Shaw and Wesnousky, 2008; Shaw, 2009).

It is common practice to use empirical regressions of fault area determined from aftershocks versus seismic moment to estimate the expected size of future earthquakes on mapped faults (e.g., Hanks and Bakun, 2002; Field *et al.*, 2008; Hanks and Bakun, 2008). Fault area is generally determined from background seismicity and earthquake aftershocks. If coseismic rupture extends below the seismogenic layer, and the depth extent increases with rupture length, the

seismic moment per unit area expected on mapped faults may be systematically overestimated for increasingly longer earthquakes, and the overestimation will systematically increase as a function of rupture length. The idea is illustrated in Figure 3 and may work to remedy the existing need of physics-based numerical models (used to estimate strong ground motions) to require rupture to extend to greater down-dip widths than are used in existing fault models in which fault widths are based on background seismicity or aftershocks.

Aseismic Deformation and the Estimation of the Rate of Seismic Moment Release along Mapped Faults

Fault displacement occurs by both seismic and aseismic processes. At one end of the spectrum the entirety of cumulative slip along a fault is accommodated by the repeated occurrence of large earthquakes, with interevent times being marked only by the continual accrual of elastic strain, akin to the concept of elastic rebound (Reid, 1910). At the other end resides the fault where the entirety of slip is accommodated by the steady continual movement of a fault in the absence of large earthquakes, generally referred to as aseismic creep (e.g., Burford and Harsh, 1980). The latter phenomenon, though well exhibited along the central San Andreas, is rare in continental environments. Within that spectrum is the manifestation of aseismic deformation temporally associated with the occurrence of earthquakes. The phenomenon was aptly illustrated in the 1987 Superstition Hills earthquake (Boatwright *et al.*, 1989; Sharp *et al.*, 1989). Surface offsets at the time of the earthquake were observed to continue aseismically and double in the weeks after the earthquake. In this case, the cumulative geologic offset being registered along the particular fault was accommodated by a mix of seismic and aseismic deformation. The phenomenon is now well recognized to be an integral part of the earthquake process, having been observed geologically and geodetically for numerous moderate to large earthquakes (e.g., Bilham and Behr, 1992; Segall and Davis, 1997; Segall *et al.*, 2000; Burgmann *et al.*, 2002; Donnellan *et al.*, 2002; Owen *et al.*, 2002).

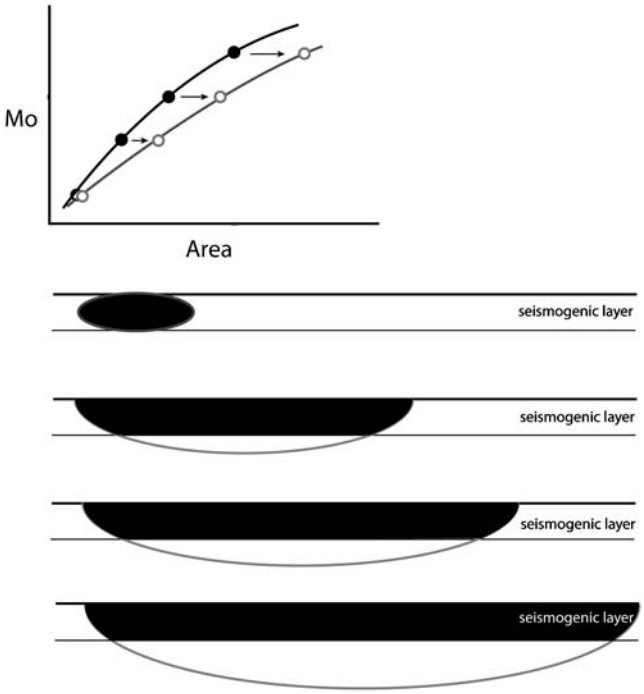

Figure 3. Contemporary regressions of fault area versus seismic moment may be overestimating the seismic moment per unit area of future earthquakes on mapped faults. The lower portion of the figure shows schematically the rupture area of four large earthquakes of increasingly greater rupture length. Black indicates the portion of rupture within the seismogenic layer and marked by seismicity or aftershocks. The gray lines depict rupture propagating below the seismogenic layer into a region of velocity-strengthening material. The region of velocity strengthening would be devoid of aftershocks. The idea is consistent with state-variable frictional laws of fault behavior (Ruina, 1983; Tse and Rice, 1986; King and Wesnousky, 2007). The upper plot schematically shows a hypothetical regression between instrumentally derived seismic moment M_0 and fault area for the four earthquakes determined from aftershocks (black line and solid dots) or from accounting for propagation to some extent below the seismogenic layer (gray lines and open dots). The black line is analogous to what is used today and implies a greater density of seismic moment per unit fault area than does the gray line for earthquakes of equivalent M_0.

Aseismic deformation may also occur contemporaneously with seismic slip. The process is most readily observed in the examination of dip-slip earthquakes in which coseismic displacement is divided between slip on a fault plane and production of fold deformation. The 1980 El Asnam, Algeria, 1983 Coalinga, and 1994 Northridge, California, earthquakes are examples of the phenomenon (King and Yielding, 1984; Stein and King, 1984; Davis and Namson, 1994). Fault slip was confined to depth, and fault displacement is recorded toward the surface not by fault slip but rather by folding. So, similar to the process of afterslip, cumulative slip registered at the surface is a result of both seismic and aseismic deformation.

The seismic moment of historical surface rupture earthquakes determined from geologic measures of surface slip is plotted as a function of the instrumentally determined seismic moment of the respective earthquakes in Figure 4. Geologic moment is computed by multiplication of geologists' measures of coseismic offset $U^{\exp}$ and surface rupture length L on the ground surface by seismologists' estimates of fault width W from seismicity and crustal rigidity μ. The data of Figure 4 show that the ratio of geologic moment to seismic moment approaches unity (slope of 1 on plot) for the largest events in the data set and also that the scatter of the data below the line of slope 1 increases inversely with seismic moment. One may infer from the observation that the lesser-sized events more commonly do not completely rupture to the surface; hence, they do not produce seismic slip across the entire fault plane. If such earthquakes represent the repeating pattern particular to a moderate-sized fault or fault segment, aseismic slip is likely to account for a portion of cumulative geologic slip measured across the surface

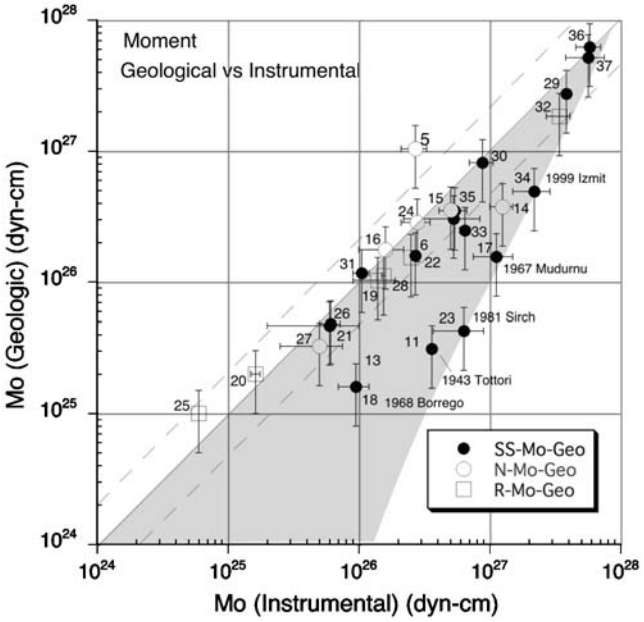

Figure 4. Geologic moment versus seismic moment for large surface rupture earthquakes. Geologic moment is computed by multiplication of geologists' measures of surface offset and surface rupture length by seismologists' estimates of fault width from seismicity and crustal rigidity. Perfect agreement of the two measures would plot on a line of slope 1. The shaded region encompasses all points on and below the line of slope 1. The scatter of data below the line of slope 1 increases inversely with M_0 and thus rupture length. Data are replotted from Wesnousky (2008). Strike-slip (SS), normal (N), and reverse (R) earthquakes are plotted with different symbols. Vertical error bars span a factor of 3 in seismic moment. Horizontal error bars represent the range of multiple estimates of seismic moment from various investigators.

expression of the fault. When viewing Figure 4 and recognizing that the plot does not include many moderate-sized earthquakes characterized by an absence of significant surface rupture (e.g., the 1983 M 6.4 Coalinga, 1994 M 6.7 Northridge, and 1989 M 6.9 Loma Prieta earthquakes), the possibility arises that there is a tendency for the percentage of slip accommodated by aseismic deformation to increase inversely to the length of the fault or fault segment producing an earthquake. The observations and assumption of repeating earthquakes, if indeed representative of the earthquake process, will lead to a systematic error in estimating the seismic moment rate from geologic slip rates. That is to say, the seismic moment rate calculated from fault slip rate assuming rupture across the entire seismogenic zone would, as an inverse function of the fault length expected to rupture, overestimate the actual seismic moment release rate.

Consequence of Observations on Prediction of Seismicity and Strong Ground Motion from Active Fault Data Sets

The observations presented in the preceding two sections allow the suggestions (1) that estimates of the seismic moment per unit area of earthquakes on mapped faults based on empirical regressions of seismic moment and aftershock area may, as a function of fault length, be systematically overestimated for large earthquakes and (2) assessments of the seismic moment rate on mapped faults determined from fault slip rates may as an inverse function of fault length be systematically overestimated. The effect of the first of these is that long-period strong ground motions may systematically be overestimated as a function of earthquake rupture length. The effect of the second may be leading to a systematic overprediction of the number of moderate-sized earthquakes in regional fault models when the return time T of earthquakes on active faults is computed with the expression $M_0^{\exp}/\dot{M}_0$. If in the context of observations presented here, the expression for return time T is rewritten as $M_0^{\exp}/\beta\dot{M}_0$ where β represents the fraction of moment rate released seismically and is taken to be a positive function of fault length, estimates of the return time T for earthquakes on smaller faults will experience a relative increase. Over a regional fault model, the effect will produce a systematic change in the predicted seismicity as expressed in a magnitude-frequency distribution plot. The manner of change is schematically illustrated in Figure 5. The resulting shift would tend to diminish or remove the bulge.

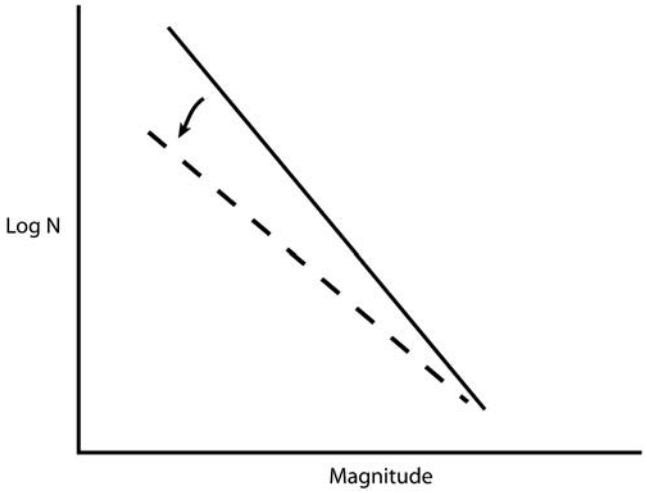

Figure 5. Schematic illustration of the sense of change that would be expected in seismicity predicted from geologic data if the return time of earthquakes on each fault is written $T = M_0^{\exp}/\beta\dot{M}_0$, where β represents the fraction of moment rate released seismically and is taken to be a positive function of fault length. The black line schematically depicts a magnitude-frequency distribution calculated from a regional distribution of faults assuming that the return time on each fault $T = M_0^{\exp}/\dot{M}_0$, whereas the dashed line includes the effect of β. Inclusion of the bias represented as β will lead to relatively longer return time T estimates (less frequent occurrence) for smaller earthquakes, respectively. The net effect will be a shift of the slope of magnitude-frequency distribution toward the dashed line.

Summary

Systematic biases in the estimation of earthquake size and return time from geologic data sets describing the length

and slip rate of active faults may arise from aseismic processes. Estimates of the seismic moment (per unit area) on mapped faults may currently be systematically overestimated as a function of fault length if large earthquakes extend below the seismogenic layer and the extent is a function of rupture length. The seismic moment rate on mapped faults determined from fault slip rate data may be systematically biased if the portion of slip accommodated by aseismic processes during earthquakes is inversely proportional to rupture length. While current observations do not prove large earthquakes rupture coseismically below the seismogenic layer nor that aseismic deformation is sufficiently ordered or of magnitude to systematically affect the prediction of seismicity over regional fault models, the observations at hand appear sufficient to suggest that an increased understanding of these parameters and the physical processes they represent may ultimately lead to more accurate and internally self-consistent estimates of seismic hazard.

Data and Resources

All data used in this note came from published sources listed in the references.

Acknowledgments

I thank Jim Brune, Paul Somerville, and Oliver Boyd for their interest and comments. This research was supported by the Southern California Earthquake Center (SCEC). SCEC is funded by National Science Foundation Cooperative Agreement EAR-0106924 and U.S. Geological Survey (USGS) Cooperative Agreement 02HQAG0008. SCEC Publication Number 1421, Center for Neotectonic Studies Contribution Number 56.

References

Aki, K., and P. Richards (1980). *Quantitative Seismology, Theory and Methods*, W. H. Freeman, San Francisco, 932 pp.

Bilham, R., and J. Behr (1992). A 2-layer model for aseismic slip on the Superstition Hills fault, California, *Bull. Seismol. Soc. Am.* **82,** no. 3, 1223–1235.

Boatwright, J., K. E. Budding, and R. V. Sharp (1989). Inverting measurements of surface slip on the Superstition Hills fault, *Bull. Seismol. Soc. Am.* **79,** no. 2, 411–423.

Burford, R. D., and P. W. Harsh (1980). Slip on the San Andreas fault in central California from alignment array surveys, *Bull. Seismol. Soc. Am.* **70,** 1233–1261.

Burgmann, R., S. Ergintav, P. Segall, E. H. Hearn, S. McClusky, R. E. Reilinger, H. Woith, and J. Zschau (2002). Time-dependent distributed afterslip on and deep below the Izmit earthquake rupture, *Bull. Seismol. Soc. Am.* **92,** no. 1, 126–137.

Davis, T. L., and J. S. Namson (1994). A balanced cross-section of the 1994 Northridge earthquake, Southern California, *Nature* **372,** no. 6502, 167–169.

Donnellan, A., J. W. Parker, and G. Peltzer (2002). Combined GPS and InSAR models of postseismic deformation from the Northridge earthquake, *Pure Appl. Geophys.* **159,** no. 10, 2261–2270.

Field, E. H., T. E. Dawson, K. R. Felzer, A. D. Frankel, V. Gupta, T. H. Jordan, T. Parsons, M. D. Petersen, R. S. Stein, R. J. Weldon, and C. J. Wills (2008). The Uniform California Earthquake Rupture Forecast, Version 2 (UCERF 3), *U. S. Geol. Surv. Open-File Rept. 2007–1437*, 96 pp.

Field, E. H., T. E. Dawson, K. R. Felzer, A. D. Frankel, V. Gupta, T. H. Jordan, T. Parsons, M. D. Petersen, R. S. Stein, R. J. Weldon, and C. J. Wills (2009). Uniform California Earthquake Rupture Forecast, Version 2 (UCERF 2), *Bull. Seismol. Soc. Am.* **99,** no. 4, 2053–2107.

Frankel, A. D., M. D. Petersen, C. S. Mueller, K. M. Haller, R. L. Wheeler, E. V. Leyendecker, R. L. Wesson, S. C. Harmsen, C. H. Cramer, D. M. Perkins, and K. S. Rukstales (2002). Documentation for the 2002 update of the national seismic hazard maps, *U.S. Geol. Surv. Open-File Rept. 02-0420*, 39 p.

Graves, R., S. Callaghan, E. Deelman, E. Field, T. H. Jordan, G. Juve, C. Kesselman, P. Maechling, G. Mehta, K. Milner, D. Okaya, P. Small, and K. Vahi (2010). CyberShake: A physics-based seismic hazard model for Southern California, *Pure Appl. Geophys. in press*.

Hanks, T. C., and W. H. Bakun (2002). A bilinear source-scaling model for $M - \log A$ observations of continental earthquakes, *Bull. Seismol. Soc. Am.* **92,** no. 5, 1841–1846.

Hanks, T. C., and W. H. Bakun (2008). $M - \log A$ observations for recent large earthquakes, *Bull. Seismol. Soc. Am.* **98,** no. 1, 490–494.

Hillers, G., and S. G. Wesnousky (2008). Scaling relations of strike-slip earthquakes with different slip-rate-dependent properties at depth, *Bull. Seismol. Soc. Am.* **98,** no. 3, 1085–1101.

King, G., and G. Yielding (1984). The evolution of a thrust-fault system—Processes of rupture initiation, propagation and termination in the 1980 El-Asnam (Algeria) earthquake, *Geophys. J. R. Astr. Soc.* **77,** no. 3, 915–933.

King, G. C. P., and S. G. Wesnousky (2007). Scaling of fault parameters for continental strike-slip earthquakes, *Bull. Seismol. Soc. Am.* **97,** no. 6, 1833–1840.

Owen, S., G. Anderson, D. C. Agnew, H. Johnson, K. Hurst, R. Reilinger, Z. K. Shen, J. Svarc, and T. Baker (2002). Early postseismic deformation from the 16 October 1999 M_w 7.1 Hector Mine, California, earthquake as measured by survey-mode GPS, *Bull. Seismol. Soc. Am.* **92,** no. 4, 1423–1432.

Petersen, M. D., T. Q. Cao, K. W. Campbell, and A. D. Frankel (2007). Time-independent and time-dependent seismic hazard assessment for the State of California: Uniform California Earthquake Rupture Forecast Model 1.0, *Seism. Res. Lett.* **78,** no. 1, 99–109.

Reid, H. F. (1910). The California earthquake of April 18, 1906, the mechanics of the earthquake, in *The State Earthquake Investigation Committee Report*, Carnegie Institute, Washington D.C.

Ruina, A. (1983). Slip instability and state variable friction laws, *J. Geophys. Res.* **88,** no. B12, 359–370.

Segall, P., and J. L. Davis (1997). GPS applications for geodynamics and earthquake studies, *Ann. Rev. Earth Planet. Sci.* **25,** 301–336.

Segall, P., R. Burgmann, and M. Matthews (2000). Time-dependent triggered afterslip following the 1989 Loma Prieta earthquake, *J. Geophys. Res. Solid Earth Planets* **105,** no. B3, 5615–5634.

Sharp, R. V., K. E. Budding, , J. Boatwright, M. J. Ader, M. G. Bonilla, M. M. Clark, T. E. Fumal, K. K. Harms, J. J. Lienkaemper, D. M. Morton, B. J. Oneill, C. L. Ostergren, D. J. Ponti, M. J. Rymer, J. L. Saxton, and J. D. Sims (1989). Surface faulting along the Superstition Hills fault zone and nearby faults associated with the earthquakes of 24 November 1987, *Bull. Seismol. Soc. Am.* **79,** no. 2, 252–281.

Shaw, B. E. (2009). Constant stress drop from small to great earthquakes in magnitude-area scaling, *Bull. Seismol. Soc. Am.* **99,** no. 2A, 871–875.

Shaw, B. E., and S. G. Wesnousky (2008). Slip-length scaling in large earthquakes: The role of deep-penetrating slip below the seismogenic layer, *Bull. Seismol. Soc. Am.* **98,** no. 4, 1633–1641.

Somerville, P. (2006). Review of magnitude-area scaling of crustal earthquakes report, URS Corp., Pasadena, California, 22 pp.

Stein, R. S., and G. C. P. King (1984). Seismic potential revealed by surface folding—1983 Coalinga, California, earthquake, *Science* **224,** no. 4651, 869–872.

Tse, S. T., and J. R. Rice (1986). Crustal earthquake instability in relation to the depth variation of frictional slip properties, *J. Geophys. Res. Solid Earth Planets* **91,** no. B9, 9452–9472.

Wells, D. L., and K. J. Coppersmith (1994). New empirical relationships among magnitude, rupture length, rupture width, rupture area, and surface displacement, *Bull. Seismol. Soc. Am.* **84,** no. 4, 974–1002.

Wesnousky, S. G. (1986). Earthquakes, Quaternary faults, and seismic hazard in California, *J. Geophys. Res. Solid Earth Planets* **91,** no. B12, 2587–2631.

Wesnousky, S. G. (2008). Displacement and geometrical characteristics of earthquake surface ruptures: Issues and implications for seismic-hazard analysis and the process of earthquake rupture, *Bull. Seismol. Soc. Am.* **98,** no. 4, 1609–1632.

Wesnousky, S. G., C. H. Scholz, K. Shimazaki, and T. Matsuda (1983). Earthquake frequency-distribution and the mechanics of faulting, *J. Geophys. Res.* **88,** no. B11, 9331–9340.

Wesnousky, S. G., C. H. Scholz, K. Shimazaki, and T. Matsuda (1984). Integration of geological and seismological data for the analysis of seismic hazard—A case-study of Japan, *Bull. Seismol. Soc. Am.* **74,** no. 2, 687–708.

Center for Neotectonic Studies
University of Nevada, Reno
Nevada 89557
wesnousky@unr.edu

Manuscript received 2 December 2009